Electronic structure of large systems: Coping with small gaps using the energy renormalization group method

Roi Baer and Martin Head-Gordon

Citation: The Journal of Chemical Physics **109**, 10159 (1998); doi: 10.1063/1.477709
View online: http://dx.doi.org/10.1063/1.477709
View Table of Contents: http://scitation.aip.org/content/aip/journal/jcp/109/23?ver=pdfcov
Published by the AIP Publishing

Electronic structure of large systems: Coping with small gaps using the energy renormalization group method

Roi Baer[a] and Martin Head-Gordon
Department of Chemistry, University of California, Berkeley and Chemical Sciences Division, Lawrence Berkeley National Laboratory, Berkeley, California 94720-1460

(Received 17 July 1998; accepted 4 September 1998)

A newly developed energy renormalization-group method for electronic structure of large systems with small Fermi gaps within a tight-binding framework is presented in detail. A telescopic series of nested Hilbert spaces is constructed, having exponentially decreasing dimensions and electrons, for which the Hamiltonian matrices have exponentially converging energy ranges focusing to the Fermi level and in which the contribution to the density matrix is a sparse contribution. The computational effort scales near linearly with system size even when the density matrix is highly nonlocal. This is illustrated by calculations on a model metal, a small radius carbon-nanotube and a two-dimensional puckered sheet polysilane semiconductor. © *1998 American Institute of Physics.* [S0021-9606(98)31046-6]

I. INTRODUCTION

The Kohn–Sham[1] version of the density-functional theory[2] (KS-DFT) in electronic structure theory has revolutionized our ability to simulate and understand processes in large condensed matter and biological systems. It has served not only as a rigorous basis for *ab initio* approximations but also as a theoretical motivation for various semiempirical approaches. One, the tight-binding semiempirical method,[3] rests on the rigorous fact that there exists a one-electron Hamiltonian with a local potential in *R*-space having well defined physical properties from which certain exact electronic observables (such as force on nuclei) can in principle be calculated.

Once a tight-binding (TB) model Hamiltonian is defined, the primary computational task is to calculate the corresponding one-electron density matrix (DM). A highly desirable property for DM calculation algorithms of large systems is that the computational load scales only linearly with system size, the so-called ''linear scaling'' property. Linear scaling approaches can be categorized in four classes: The divide and conquer[4–6] orbital minimization,[7–16] Chebyshev expansion,[17–22] and density-matrix minimization.[23–27] The reader is referred to a recent comprehensive review[28] for a comparison of the methods and additional references. These methods are not limited to TB models, and are equally useful in more exact forms of self-consistent field (SCF) DFT, such as local density and generalized gradient approximations. Within SCF theory the methods need be supplemented with linear-scaling Hamiltonian-buildup techniques.[29–32] The linear scaling methods, although very new have already made significant impact in many physical and chemical problems.[33–37]

There is, however, a basic limitation of these methods, because they all exploit the ''near sightedness principle'' [27] or the exponential decay of density matrix (DM) correlations in real space[38–44] (loosely referred to as DM sparsity). There are interesting systems such as metals, where the DM is not sparse because two point DM correlations decay only algebraically.[42,44] Even for nonmetals, such as semiconductors, when the band gap is small, and the DM has long-range correlation ranges in which case only for very large systems does DM sparsity actually show up. Linear scaling for these systems, although possible in principle, is unachievable in practice.

Certain systems can have a vanishing energy gap between the highest occupied orbital (HOMO) and the lowest unoccupied orbital (LUMO) with finite DM range. This is seen in Anderson-disordered systems[45] and when noninteracting parts of a system have ''accidental degeneracy.'' Such a situation also happens because of symmetry induced degeneracy, as for Si vacancies which exhibit a D_{2d} Jahn–Teller distortion.[46,47] In these situations, although the DM is in principle sparse the need to resolve the degeneracy at the Fermi level leads to numerical difficulties.[21] However, it is the former case, where in addition to a small gap the DM correlation range is large that poses the greater difficulty. When the DM is nonsparse it is in principle impossible to perform controlled linear scaling calculations.

The DM is the zero temperature limit of the Fermi dirac density matrix (FD-DM). This is a common view in solid-state physics. The finite, high-temperature FD-DM has correlation-lengths approximately proportional to a small power (typically between 0.5 and 1) of the inverse temperature.[38–44] Thus the FD-DM correlation range is controlled by selecting a large enough finite temperature. If the HOMO–LUMO gap is large, the FD-DM approximates the DM excellently even at these high temperatures. However, when the gap is very small, the temperature of the FD-DM must be, respectively, reduced and its range becomes large.

It was proposed by Nicholson *et al.*[48] that a zero tem-

[a]Permanent address: Dept. of Physical Chemistry, the Hebrew University, Jerusalem 91904, Israel.

perature limit can be reached by extrapolation within the recursion method of Haydock.[49] However, in a linear scaling implementation of this approach by Wang *et al.*[50] a local interaction zone was used. When the DM range grows as the temperature is lowered (as happens in metals and semiconductors) the system is not anymore ''near-sighted'' and so far away features can affect the energy. Thus an extrapolation from high to low temperature based on calculations in a local zone is not reliable as it assumes a homogeneity not necessarily present in the system.

This paper attempts to contribute to the effort of overcoming these limitations: We try to enhance the capability and scope of linear scaling to the difficult cases of nonsparse DMs. This also gives effective tools to deal with the related problem of other gapless or small gapped systems. We develop an alternative approach to the ''low-temperature limit'' of the DM. Instead of taking the limit we relate the DM to a *telescopic sum of terms*. By construction, each term focuses on an increasingly smaller energy interval around the Fermi level. We demonstrate that each term is sparse if described in a space spanned by coarse grained basis functions. We give the prescription to create these coarse grained spaces and sparse matrices.

The method is based on a renormalization-group (RG) point of view, where DM correlations are described in varying length and energy scales.[51] Indeed, we demonstrate that in a metallic band the range of the DM is an invariant of the RG transformation, a property attributed by RG theory to infinite correlation lengths.[51,52] The numerical RG approach presented here, called the energy renormalization group (ERG), is different from conventional real-space RG in which a super block is constructed from a given number of blocks in real space.[53] In ERG, it is the energy which is rescaled by a constant factor at each step. This overcomes the problems of block boundary conditions noted by White *et al.*[54] We use Chebyshev expansion methods[55] for calculating the Fermi-Dirac (FD) matrix[17–19] and our method for performing a renormalization step is inspired by filter-diagonalization.[56,57]

In Secs. II and III we discuss the theory of the ERG approach as applied to a tight-binding model of the system Hamiltonian. We use a simple model for a metal to show many characteristics The theory can also be formulated for SCF/DFT applications and work in these directions is currently under way. In Sec. IV we present two examples of ERG at work: A simple model of a metal and a two-dimensional small gap semiconducting puckered sheet polysilane.

II. BACKGROUND

A. A functional approach

The electronic structure problem is the calculation of ground-state expectation values within a tight-binding model (TBM). The TBM is usually defined without reference to basis functions, however, for convenience of formalism, suppose that these exist and are localized functions $a(r)$. Using the sparse overlap matrix $S_{ab}=\langle a|b\rangle$ we can define orthonormal basis functions $\tilde{a}(r)=\Sigma_b(S^{-1/2})_{ab}b(r)$ with which the Hamiltonian $\hat{H}$ is represented by the sparse matrix TB Hamiltonian $H_{ab}=\langle\tilde{a}|\hat{H}|\tilde{b}\rangle$.

The functional approach describes the central quantity of the electronic structure problem, the one electron density operator as a *function of the Hamiltonian*. In the electronic ground state the electron density operator is defined using the Heaviside function $\theta(\epsilon)$ (equal to 1 when $\epsilon>0$ and 0 otherwise) by

$$\hat{\rho}=\theta(\mu-\hat{H}). \tag{1}$$

This operator is represented by the DM $\rho_{ab}=\langle\tilde{a}|\hat{\rho}|\tilde{b}\rangle$. The value of the Fermi level μ in Eq. (1) is determined by the condition $tr\rho=N_e$ where $2N_e$ is the number of electrons in the system. The ground-state energy is

$$E=tr\{H\rho\}. \tag{2}$$

In the functional approach, it is convenient to define also the Fermi-dirac (FD) density operator at inverse temperature β

$$\hat{F}_\beta=F_\beta(\hat{H})=\frac{1}{1+e^{\beta(\hat{H}-\mu)}}. \tag{3}$$

The ground-state density is the zero-temperature limit of the FD density

$$\lim_{\beta\leftarrow\infty}\hat{F}_\beta=\hat{\rho} \tag{4}$$

Equation (4) is the conventional view: The ground-state density of metals is the zero-temperature limit of the FD density.

B. The Chebyshev expansion

The functional approach, where various quantities are formulated as functions of the Hamiltonian, is useful because an extremely economical and flexible way to calculate these functions is available in terms of a Chebyshev expansion.[55] Notice that, unlike $\hat{\rho}$, which is a nonanalytical function of the Hamiltonian, $\hat{F}_\beta$ can be represented by a uniformly convergent Chebyshev series[17,18] of length P.

In their matrix representations we write

$$F_\beta(H)\approx\sum_{n=0}^{P-1}a_n(\beta,\mu)T_n(H_N), \tag{5}$$

where $T_n(\cos\theta)=\cos n\theta$ are Chebyshev polynomials of the variable $x=\cos\theta$ and

$$H_N=(H-\overline{E})/\Delta E,$$

$$\Delta E=(E_{\max}-E_{\min})/2,\quad \overline{E}=(E_{\max}+E_{\min})/2. \tag{6}$$

Here, $E_{\min}$ and $E_{\max}$ are the smallest and largest eigenvalues of the Hamiltonian matrix. The expansion coefficients a_n are given by

$$a_n=\frac{2}{\pi(1+\delta_{n,0})}\int_0^\pi f(\theta)\cos n\theta d\theta, \tag{7}$$

where $f(\theta)=F_\beta(\Delta E\cos\theta+\overline{E})$. Numerical evaluation of this integral is efficiently and accurately performed using fast Fourier transform (FFT) methods.

The operation of F_β on a wave function represented by the column Ψ is carried out using the Chebyshev recursion relation

$$T_{n+1}(H_N)\Psi \equiv \Psi_{n+1} = 2H_N\Psi_n - \Psi_{n-1}. \tag{8}$$

Note that only three vectors need be stored at once during the calculation.[55] The entire FD-DM can be calculated column by column by successively expanding on all unit vectors in the representation space.[17] The fact that the matrix can be calculated column by column means that the computation is inherently parallelizable and that the entire FD-DM need never be fully stored. In order to use the Chebyshev methods efficiently, the representation of matrices and vectors should be such as to enable full exploitation of their sparsity. The ERG calculations we show here are based on a binary tree representation,[19] which facilitates the locality of the various matrices and vectors. Other sparse methods may also be used.

For precision 10^{-D}, the Chebyshev expansion length is[19]

$$P = \tfrac{2}{3}(D-1)\beta\cdot\Delta E. \tag{9}$$

If the treated system is not a metal, so that a HOMO–LUMO gap $\delta\epsilon$ exists, we approximate the DM to precision 10^{-D} by a FD distribution with a finite β given by[19]

$$\beta\cdot\delta\epsilon/2 \geqslant D\cdot\log(10), \tag{10}$$

One can see qualitatively what happens as the gap $\delta\epsilon$ diminishes (and the system gradually becomes a metal). The inverse temperature parameter must grow for Eq. (10) to hold. But by Eq. (9) this will cause an increasingly larger Chebyshev expansion. Suppose now that the Hamiltonian is represented by a matrix H_N in which the matrix elements are zero beyond a cutoff radius r_c. Then H_N^P must have no nonzero elements beyond a radius Pr_c. Thus the range of the DM in this case is rigorously bounded by

$$R(\hat{F}) < P\cdot r_c \approx \tfrac{2}{3}\beta\Delta E(D-1)r_c. \tag{11}$$

This result shows in a very general way that the DM of any system at positive temperatures *is always sparse* and the range is bounded by a term which grows linearly with inverse temperature. This bound may grossly overestimate the DM range in many cases, especially when P is not too large. This is because the Hamiltonian is not only banded but exhibits an overall decay as the cutoff radius is approached. An approximate way to take this into account is given in Ref. 41 leading to an estimate of the DM range as $R(F) < A\beta^{1/2}$. This estimate agrees, as it should, with the high-temperature behavior given by a classical correlation range. A striking example of the overestimation of Eq. (11) is observed for gapless disordered systems at the localization regime. This does not, however, exclude the existence of systems exhibiting a DM range proportional to $1/T$ even as $T\to 0$. Indeed, it was recently found by Goedecker[28,44] and independently by Ismail–Beigi *et al.*[43] that a simple metal exactly exhibits this decay behavior at low temperatures (when $\beta \geqslant \epsilon_F$). Furthermore, it was proved[43,44] that the DM range decays only algebraically at $T=0$ (proportional to r^{-2}). Based on the work of these authors it can be deduced that semiconductors may be in the intermediate region with correlation lengths decaying faster than $1/T$ but slower than $1/T^{1/2}$.

The conclusion is that for small gapped systems, semiconductors and metals, the DM correlations may either be very large or may grow indefinitely as the temperature is lowered. This severely limits the ability of pure *R*-space based methods to effectively treat these systems. The ERG method presented now attempts to treat this problematic point in linear scaling methods.

III. THE ERG METHOD

A. Principles of the method

The DM is the zero-temperature limit of the FD-DM [see Eq. (4)] and for metals, as the temperature in the FD-DM is lowered, the range of FD matrix correlations increases [Eq. (11)] and the matrix becomes nonsparse. This nonsparsity tells us that the way we think and represent the DM is actually problematic. An alternative view of the relation between the FD-DMs and the DMs is needed.

More useful is to associate the DM as a series, *sum of terms*, instead of a limit. The series we consider is telescopic with temperature decreasing in each term by a factor $q>1$

$$\begin{aligned}\hat{\rho} &= \hat{F}_{\beta_0} + (\hat{F}_{\beta_1} - \hat{F}_{\beta_0}) + (\hat{F}_{\beta_2} - \hat{F}_{\beta_1}) + \cdots \\ &= \hat{F}_{\beta_0} + \hat{\Delta}_1 + \hat{\Delta}_2 + \cdots .\end{aligned} \tag{12}$$

What is the meaning of this equation? We view the DM as composed of a high-temperature (small β_0) FD-DM plus additional terms Δ_n $n=1,2...$ gradually correcting for lower temperatures. Each term corrects for a temperature scale lower by the factor q from that of the previous term, so that $\beta_n = q^n\beta_0$.

Let us now study the properties of the operators in the series of Eq. (12). We do this in two spaces: In *R*-space and in energy space. To demonstrates our arguments, we consider a one-dimensional (ID) system of N sites with a nearest-neighbor one-electron Hamiltonian

$$H = 2\sum_i a_i^+ a_i - \sum_{\langle i,j\rangle} a_i^+ a_j. \tag{13}$$

Here $i=1\cdots N$ indexes the sites and j is a nearest neighbor site.

In the *R*-space localized basis the matrix representing $\hat{F}(\beta_0)$ is strongly localized because β_0 is chosen small [see Eq. (11)]. This is seen in Fig. 1 for our model system, where a typical column of the FD matrix is plotted. According to Eq. (12), the long-range DM correlations quenched by β_0 are introduced step by step while gradually cooling the system successively by the renormalization factor q. This gives DM corrections $\hat{\Delta}_n$ $(n=1,2,...)$, which are increasingly delocalized in *R*-space (see Fig. 2).

Next, consider energy space. The operators of Eq. (12) are all functions of the Hamiltonian, so they are simultaneously diagonalized in the energy eigenstate basis. The eigenvalues of the operators as a function of the energy of the eigenstates (for convenience, we scaled the energy to the interval [0,1]) are shown in Fig. 3. We show the FD distri-

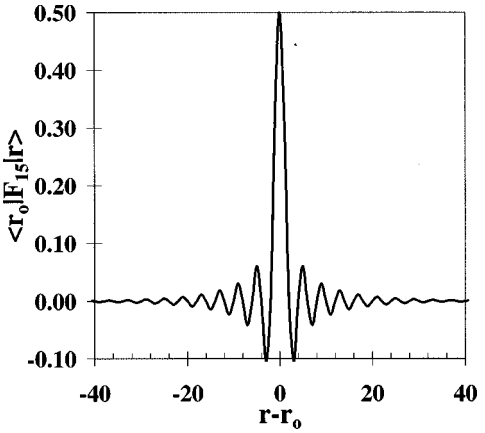

FIG. 1. A column of the FD-DM for $\beta=15$ for the model defined in Eq. (13), with $\mu=2.0$.

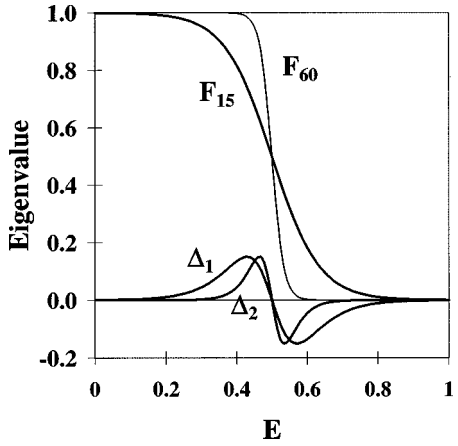

FIG. 3. The eigenvalues of the first three terms in Eq. (12) contributing to the DM when $\beta_0=15$ and $q=2$. The sum of these terms gives a low-temperature F_{60} (eigenvalues shown as thin line).

bution at a high temperature ($\beta_0=15$) and then two Δ contributions each with β increasing by the factor $q=2$. The higher β becomes, the smaller the supporting energy interval (where eigenvalues are non-negligible). Each of the terms in the sum of Eq. (12) is thus supported by successively smaller dimensional Hilbert subspace.

To summarize: In *R*-space, the $\hat{\Delta}_n$ represents increasingly larger length scales, while in energy space they are supported by successively smaller dimensional Hilbert spaces. These Hilbert spaces can therefor be spanned by longer ranged *R*-space basis functions, that is by a *coarse-grained basis*.

What we now need is a general method to create the coarse-grained basis and the representation of the Hamiltonian and other operators in the coarse grained Hilbert space. But before we turn to this crucial issue, let us make an additional remark as to the way we actually use Eq. (12) in computations. While it is appealing to think in terms of Eq. (12), and indeed we shall do so in the rest of this section, it should be kept in mind that we never explicitly *create the matrix* corresponding to $\hat{\rho}$ since it is nonsparse and, therefore, computationally prohibitive. Instead, we use Eq. (12) in expectation value expressions, for example, the ground-state energy of Eq. (2) becomes

$$E=tr\{\hat{H}\hat{F}_{\beta}\}+tr\{\hat{H}\hat{\Delta}_1\}+tr\{\hat{H}\hat{\Delta}_2\}+\cdots . \tag{14}$$

(note, that we can write an analogous equation for any electronic expectation value). Here, the trace operations are performed separately for each term in the corresponding coarse grained space. The full DM is thus never explicitly needed.

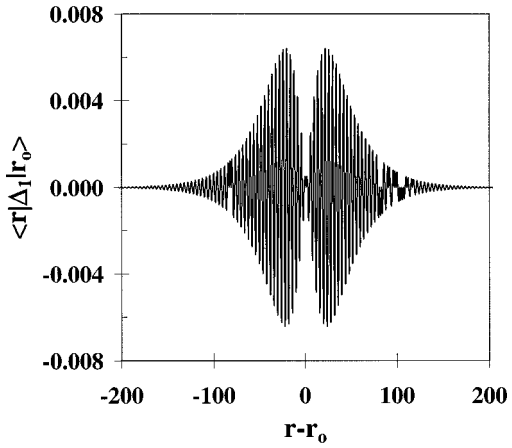

FIG. 2. A typical column of the matrix Δ_1 (in a series with $\beta_0=15$ and $q=3$) for the model defined in Eq. (13), with $\mu=2.0$.

B. The ERG coarse graining step: A functional approach

We now turn to the issue of constructing the coarse-grained Hilbert spaces. The ERG is recursive so what we need is a matrix representation of the Hamiltonian (and any other operator whose expectation value we wish to calculate) in an orthogonal basis of the $(n+1)$th coarse-grained Hilbert space. These matrices are to be calculated from the corresponding ''known'' matrices of the nth space.

We define the following function of the Hamiltonian, loosely called the Fermi level density of states (DOS) ($n=0,1,...$)

$$G^{(n)}(\hat{H})=\frac{\partial}{\partial\mu}\hat{F}_{\beta_n}=\beta_n\frac{e^{\beta_n(\hat{H}-\mu)}}{(1+e^{\beta_n(\hat{H}-\mu)})^2}. \tag{15}$$

The action of the operator $\hat{G}^{(n)}$ on a given vector, is made apparent by examining its eigenvalues in Fig. 4. When $\hat{G}^{(n)}$ operates on any vector in the nth space, it zeros components of energy outside the interval $[\mu-M\beta_n^{-1},\mu+M\beta_n^{-1}]$ (M is a number of order 10). Thus $\hat{G}^{(n)}$ is a pseudo-projector onto the $(n+1)$th space. We do not have enough experience to formulate accurate guidelines on the desired form of G. Several forms for this pseudo-projector were tried. For example, a properly chosen Gaussian form $G=A\exp(-\alpha(H-\mu)^2)$ can also be used. However, to our (as yet limited) experience, the best results are achieved with the form given by Eq. (15).

The matrix $G^{(n)}_{a,b}=\langle\tilde{a}^{(n)}|\hat{G}^{(n)}|\tilde{b}^{(n)}\rangle$ [where the $N^{(n)}$ basis functions of the nth space are $\tilde{a}^{(n)}(r)=\langle r|\tilde{a}^{(n)}\rangle$] can be calculated column by column using a length P Chebyshev ex-

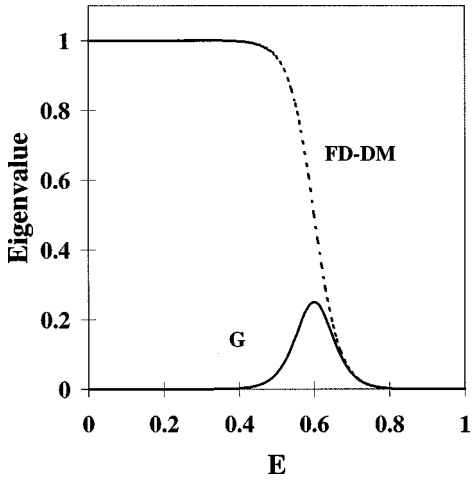

FIG. 4. The eigenvalues of the FD-DM and the filter G for $\beta=40$ and $\mu=0.6$.

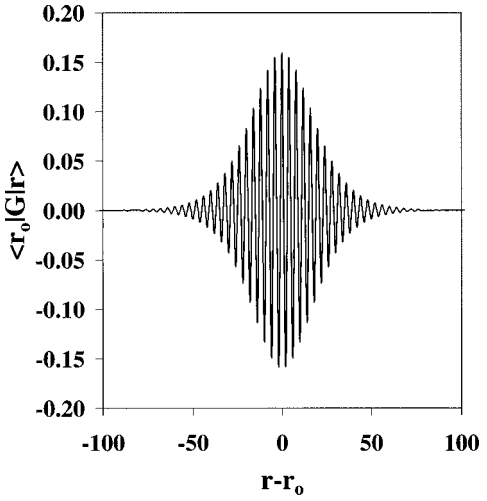

FIG. 5. A column of the matrix G defined in Eq. (15), with $\mu=2.0$ and $\beta=15$. This column is much less localized around $\mathbf{r}-\mathbf{r}_0=0$ than the Hamiltonian. The range is determined by β. Columns such as these form the basis functions for the coarse grained space.

pansion in the same way the FD-DM columns are computed, (but with different expansion coefficients). $G^{(n)}$ is highly singular, and its rank is the dimension of the coarse grained $(n+1)$th space, $N^{(n+1)}$. The DOS at the Fermi level, $tr\{G^{(n)}\}$, serves to estimate $N^{(n+1)}$ as $M\beta_n^{-1}tr\{G^{(n)}\}$. A precise method for determining $N^{(n+1)}$ will be given below. Note an important difference between the ERG method and traditional lattice RG: The dimension of the coarse-grained space is not imposed, *it is determined* by the DOS of the system.

Since $\hat{G}^{(n)}$ is obtained by a finite number of Hamiltonian operations, every column of $G_{a,b}^{(n)}$ represents a localized function $\Sigma_b G_{a,b}^{(n)}\tilde{b}^{(n)}(r)$. To create a basis for the $(n+1)$th Hilbert space, we select $N^{(n+1)}$ columns of $G_{a,b}^{(n)}$, as described in subsection 0, and arrange them in a rectangular $N^{(n)}\times N^{(n+1)}$ matrix, designated $\mathcal{G}_{ba}^{(n)}$. On the average, one column is selected out of every $N^{(n)}/N^{(n+1)}$ columns representing spatially close functions (according to an algorithm we describe in subsection 0). The $(n+1)$th space is spanned by the functions $|a^{(n+1)}\rangle=\Sigma_b|\tilde{b}^{(n)}\rangle\mathcal{G}_{ba}^{(n)}$, and the coarse grained Hamiltonian matrix is formally given by

$$H^{(n+1)}=(S^{(n+1)})^{-1/2}\times[\mathcal{G}^{(n)}]^T\times H^{(n)}\times\mathcal{G}^{(n)}\times(S^{(n+1)})^{-1/2}, \tag{16}$$

where $S^{(n+1)}=[\mathcal{G}^{(n)}]^T\mathcal{G}^{(n)}$ is the coarse-grained overlap matrix. Equations analogous to Eq. (16) can be used to define the matrix representation of any other one electron operator we may be interested in.

Theoretically, it is possible to use Eq. (16) directly in calculation. However, we have found that the intermediate matrix $(S^{(n+1)})^{-1/2}$ is much less sparse than the final result $H^{(n+1)}$. It is, therefore, of considerable value to calculate $H^{(n+1)}$ directly from $H^{(n)}$ and $\mathcal{G}^{(n)}$. In the Appendix we show that the following series:

$$B_{k+1}=(B_k-3)B_k^2/4,$$
$$A_{k+1}=A_k-(A_kB_k+B_kA_k)/2+B_kA_kB_k/4, \tag{17}$$

with $k=0,1,...$, $B_0=(\alpha S^{(n+1)}-1)$, $A_0=\alpha[\mathcal{G}^{(n)}]^TH^{(n)}\times[\mathcal{G}^{(n)}]$, and $\alpha^{-1}=N^{(n+1)}\max_{i,j}|[S^{(n+1)}]_{i,j}|$ converge quadratically to the limits:

$$B_k\to 0,$$
$$A_k\to H^{(n+1)}, \tag{18}$$

within order 10 iterations depending on the condition number of $S^{(n+1)}$. Equation (17) converges to a matrix representing the Hamiltonian in a orthonormal basis of the coarse grained Hilbert space. This is done without explicitly orthogonalizing the coarse grained basis functions.

Once a new Hamiltonian matrix is constructed, its eigenvalue range should be accurately determined by calculating its largest and smaller eigenvalues (using a Lanczos method, for example). The resulting energy interval may not be exactly a factor q smaller than the parent interval, however, in all examples we have examined, the deviations were small and did not significantly affect the overall performance of the method.

In R-space a column of G is shown in Fig. 5. Such a column is a basis function of the nested coarse grained Hilbert space.

In subsection 0 we discuss a general algorithm for selecting the basis functions. But before we turn to that general case let us consider a simple decimation algorithm here. We performed two ERG steps, starting with $\beta_0=15$ we calculated the matrix G and constructed $\mathcal{G}$ by 1:3 decimation (that is, keeping every third column of G). Other decimation ratios are also possible in principle in correspondence to the inverse temperature β_0 and to the density of states near the Fermi level [through Eq. (15)]. In Fig. 6 we consider the R-space behavior of a column of the DM in three energy and length scales. The column corresponding to a high temperature ($\beta=15$) FD-DM is shown in (i). After an ERG step a new Hilbert space is constructed where the energy scale has been renormalized by a factor of 3. Because of the 1:3 decimation, the length scale in this space has also changed by a

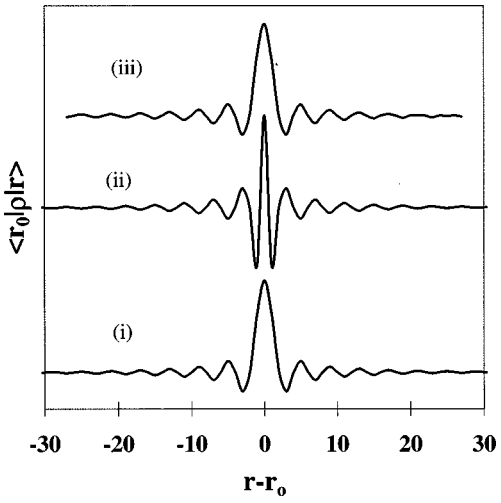

FIG. 6. A column of the FD-DM at three consecutive ERG steps for the model of Eq. (13) with $\mu=2.0$. (i) Initial: $\beta_0=15$. (ii) After first ERG step (with $q=3$). (iii) After second ERG step. Note: In each iteration length scales by a factor of 3 since we use 1:3 decimation.

factor of 3. In (ii) we show the *R*-space behavior of the column of the FD-DM. This FD-DM which corresponds to a lower temperature ($\beta=45$) looks almost the same as the previous column. In the next ERG step the energy scale has once again been reduced by an additional factor of 3. In (iii) the column of the FD-DM corresponding to very low temperature ($\beta=135$) and still looks similar to the columns of the previous ERG steps. We conclude from this figure that the decay length of the FD-DM is an invariant of the ERG transformation. This is typical in RG theory for infinite correlation lengths since they have no definite length scale.

C. Selecting basis of the nested Hilbert space

We now describe a general algorithm designed to enable the construction of $\mathbb{G}^{(n)}$ from $G^{(n)}$. Viewing $G^{(n)}$ as a set of $N^{(n)}$ columns, spanning a space $V^{(n)}$, $\mathbb{G}^{(n)}$ is a subset of size $N^{(n+1)}$ which spans $V^{(n)}$ as closely as possible under the constraint that $Cond(\mathbb{G}^{(n)})\approx 10^{D/2}$ (the condition number of $\mathbb{G}^{(n)}$) where 10^{-D} is the precision. This constraint ensures $Cond(S^{(n+1)})\approx 10^{D}$, which is needed to represent the nested space to precision 10^{-D}.

If it were not for linear scaling, we could easily use the well known singular value decomposition (SVD) to form a satisfying solution for this problem. However, like diagonalization, the SVD method will create nonlocal columns and thus will not scale linearly with $N^{(n)}$. Thus, what is needed here is an algorithm which *does not destroy the sparsity of the columns of G*. The most straightforward way to achieve this is by a selection process: We do not change any column, we only determine which column is kept and which is ''thrown away.'' A heuristic algorithm for this problem has been developed in Ref. 58 (to our knowledge there is no full-proof algorithm available, however, it is our experience that this algorithm is satisfactory). Because it does not combine or compare columns which are nonoverlapping, it is of numerical complexity $O(N^{(n)})$. The algorithm is:

1. For all k ($k=1\cdots N^{(n)}$) calculate the kth column of $G^{(n)}$ denoted $\boldsymbol{\nu}_k$. If $k=1$ (the first column) add it to $\mathbb{G}^{(n)}$, if $k>1$ perform steps 2–6 to update $\mathbb{G}^{(n)}$.

2. Identify all the columns which are currently in $\mathbb{G}^{(n)}$ and that have nonzero overlap with $\boldsymbol{\nu}_k$. Assume $L-1$ such columns exist (L is independent of system size, related only to the range of the basis functions).

3. Arrange the columns and $\boldsymbol{\nu}_k$ in a matrix C of dimensions $N^{(n)}\times L$ and calculate the $L\times L$ matrix $S=C^TC$.

4. Determine the singular value decomposition (SVD) of S: $S=Uw\nu^T$ where ν and U are orthogonal matrices and the w is diagonal with elements $w_1\geqslant w_2\geqslant\cdots\geqslant w_L\geqslant 0$. Locate the largest integer r (the rank) with $w_1/w_r<10^D$.

5. Zero the last $L-r$ rows of the matrix ν^T, yielding a new matrix ν' and perform a QR factorization with pivoting: $\nu'\Pi=QR$, where Π is a permutation of columns.

6. Replace the $L-1$ columns of $\mathbb{G}^{(n)}$ from which C was built by the first r columns of $C\Pi$.

The dimension $N^{(n+1)}$ of the coarse grained space is the final number of columns in $\mathbb{G}^{(n)}$. The number of electrons in this space is

$$N_e^{(n+1)}=N_e^{(n)}-tr\{\hat{F}_{q^n\beta}\}, \tag{19}$$

$N_e^{(n)}$ may be nonintegral if μ is inaccurately known.

With each iteration the dimension of the matrices decreases and the energy range collapses to the Fermi level μ. For a finite system the computation terminates after f iterations, when the dimension $N^{(f)}$ is small enough so the eigenvalues $\epsilon_i^{(f)}$ of $H_{ab}^{(f)}$ can be efficiently determined by numerical diagonalization. The series of Eq. (14) is terminated after f steps, where the last term is defined by (other terms were defined above)

$$tr\{\hat{H}\hat{\Delta}_f\}=\sum_{i=1}^{N^{(f)}}\{F_{\tilde{\beta},\tilde{\mu}}(\epsilon_i^{(f)})-F_{\beta_{f-1},\mu}(\epsilon_i^{(f)})\}\epsilon_i^{(f)}. \tag{20}$$

In this expression μ is the initial guess for the Fermi level which was used throughout the calculation. The quantity $\tilde{\mu}$ is a corrected Fermi level adjusted, together with $\tilde{\beta}$ so the following relation is maintained

$$\sum_{i=1}^{N^{(f)}}F_{\tilde{\beta},\mu}(\epsilon_i^{(f)})=N_e^{(f)}+\sum_{i=1}^{N^{(f)}}F_{\beta_f,\mu_0}(\epsilon_i^{(f)}), \tag{21}$$

$\tilde{\beta}$ is taken much larger than the inverse HOMO–LUMO gap (known after the diagonalization) but otherwise arbitrary.

Since the range of the FD-DM is roughly proportional to $\beta^{1/2}$, the numerical work in the ERG method is proportional to $P^{d/2+1}$ (see Ref. 38) where d is the number of extended spatial dimensions of the nuclear lattice. P should be chosen small, yet it must be large enough to achieve a significant reduction in the number of Hilbert-space dimensions at each iteration. The method is most effective when high DOS peaks are situated away from the Fermi level. The numerical work as a function of system size N scales near linearly as $N\log N$, the factor $\log N$ reflects the increase in number of iterations.

TABLE I. Renormalized parameters at the different iterations for a 16 000 site 1D metal.

Iteration	n	0	1	2	Diag.
Space dimensions	$N^{(n)}$	16 000	1692	298	89
No. of electrons	$N_e^{(n)}$	16 000	1660.6	265.5	−36.3
Energy range	ΔE_n	2.00	0.31	0.06	0.01
Inv. temperature	β_n	15	94	531	'∞'
Hamiltonian range	$R_n(H)$	3	73	55	89
FD-DM range	$R_n(F)$	132	165	120	89
Energy contribution	$\mathrm{tr}\{H^{(n)}\Delta^{(n)}\}$	5884.48	−32.75	−1.23	−36.42

IV. THE ERG METHOD AT WORK

The ERG method is a recursive method where the electronic structure problem is reformulated at each iteration, and a relevant contribution to the calculated observables is extracted at every scale.

In this section we describe in detail the steps of ERG as applied to the model of Eq. (13). We start with an enormous system of $N=16\,000$ sites. With present computing capabilities it is mandatory to treat such a large system with sparse matrix methods. Here, however, the DM is nonsparse: The matrix is too huge to even fit in computer memory.

The ERG method enjoys several advantages that allow not only to compute ground-state expectation values for this system, but also do it in a way which scales almost linearly with system size. First, ERG never computes the DM. This is because we never actually perform the summation shown in Eq. (12). Instead we sum over the results of trace operations [Eq. (14)], each trace performed in an appropriately coarse grained space. Next, computationally intense parts of the ERG computation can be parallelized. We will discuss this issue in the next section.

A. The ERG steps

We start with the full system Hamiltonian matrix, which is incredibly sparse: Only the main diagonal and the two sub-diagonals, one above and one below it are nonzero. We compute the columns of the matrix F_{β_0} assuming $\mu=2.01$ (we do not assume an exact knowledge of the value of the Fermi energy, which is 2.000). A Chebyshev series length of $P=80$ is imposed throughout the calculation. We aim at a precision of five digits, thus $D=5$. The initial energy range of the Hamiltonian is $\Delta E=2$ and using Eq. (9) we see that $\beta_0=15$.

We do not need to store the columns of F_{β_0}: They are used only to compute the trace $tr\{F_{\beta_0}H\}$ in Eq. (14) and $N-N^{(1)}=tr\{F_{\beta_0}\}$—the number of electrons already accounted for. This is also true for a SCF-DFT method where only the short-ranged part of the DM is needed to compute the electronic density (or forces on ions etc.).

The two functions F_{β_0} and $G^{(0)}$ are calculated using the Chebyshev method, where the computationally intensive part is the repeated application of the Hamiltonian to a vector. This part is identical in the two calculations and so a speedup factor of close to 2 is gained when both are calculated simultaneously. The values of parameters in the coarse-grained spaces during the ERG are shown in Table I. We see that of the $N^{(0)}=16\,000$ columns of $G^{(0)}$ only $N^{(1)}=1692$ columns survived selection and are kept in $\mathbb{G}^{(0)}$. Thus the coarse grained space has a dimension of almost a factor of 10 smaller than that of the original space. Since the system is one-dimensional, this is also the approximate relation between the length scales: We know that the 1692 basis functions cover the same amount of R-space that the original 16 000 basis functions did. On the average, the length has, therefore, been renormalized by a factor of about 10. For systems with dimensionality larger than one, the length scale is harder to define.

Using Eq. (17) we construct the representation of the Hamiltonian $H^{(1)}$ in the coarse grained space. It is found in Table I that the energy range of this Hamiltonian is a factor of $q=6$ times smaller than the original energy range.

Now we wish to determine the range $R(H^{(1)})$ of the Hamiltonian $H^{(1)}$. In general the range $R(H)$ of a matrix H is defined as the distance beyond which the matrix element of H between any two points is negligible. A precise statement is

$$R(H)=\min_R\{|\mathbf{r}-\mathbf{r}'|>R\Rightarrow|\langle\mathbf{r}|H_N|\mathbf{r}'\rangle|<10^{-D}\},$$

where H_N is defined in Eq. (6) and D is the precision in terms of number of digits. We see in Table I that the range of Hamiltonian $R(H^{(1)})$ is 72 renormalized length units. Remember that the length of the system is $N^{(1)}=1692$ renormalized units so, $R^{(1)}\ll N^{(1)}$ and the Hamiltonian matrix is very sparse. The range of the FD-DM calculated in the 0th space is $R(F^{(0)})=132$.

The renormalized values of the parameter for the third ERG step can also be found in Table I. Finally we arrive at a nonsparse Hamiltonian which is fully diagonalized at the last step. Two ''strange'' looking numbers are apparent in the table. These are: The negative number of electrons and the large energy correction: The first results from the incorrect (too large) guess we used for the Fermi level and the second from correcting for this using Eq. (21).

Performance of the ERG method as a function of system size is shown in Fig. 7. CPU time scales quasi linearly, $\sim N(\log N)^2$ (the additional factor of $\log N$ is due to the tree-code implementation[9]). Crossover is at $N\approx 4000$ for this single processor Cray C90 calculation. 60% of CPU time was consumed by the first iteration, sufficient to converge insulators with a gap $\delta\epsilon=1$ [Eq. (10) with $\beta=15$].

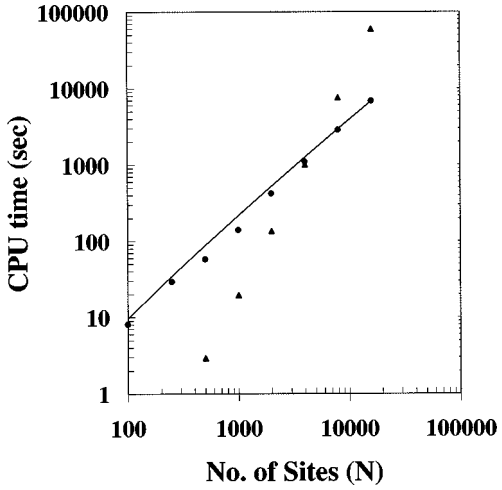

FIG. 7. ERG ($D=5$, dots) and standard diagonalization (triangles) CPU time for an energy calculation vs number of sites in the TB model of Eq. (13). Line depicts ideal asymptotic $N(\log N)^2$ scaling.

B. 1D example: A metallic carbon nanotube

The ERG method was applied to (3,0) carbon nanotubes of varying lengths, predicted to be metals,[59] using a TB Hamiltonian of Ref. 60, without the Hubbard-type correction for electron correlation. Nuclear position was not optimized (C–C distance was set to 1.49 Å prior to rolling the tube along its axis). The Chebyshev expansion lengths used were $P=80$. Performance times are shown in Fig. 8 for $D=6$ accuracy. The ERG method becomes more efficient than diagonalization based calculation at around 200 carbon atoms for a single processor on a Cray T3E.

The Chebyshev expansion length within the ERG method, of $P=80$ terms, should be compared to an expansion length of thousands, growing with system size, that would have been needed to resolve the HOMO–LUMO gap using naively the conventional Chebyshev scheme.[17,19] Because the DM is highly nonlocal in these metallic systems, similar difficulties are also expected in the direct minimization methods.[23,24]

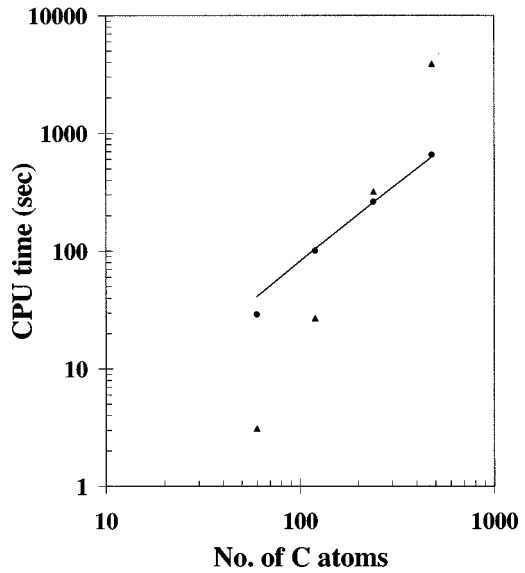

FIG. 8. CPU time for an energy calculation vs number of atoms in a metallic (3,0) carbon nanotube. Triangles: Energy calculation based on diagonalization. Filled circles: High accuracy ($D=6$) ERG calculation. Line is a $N(\log N)^2$ line.

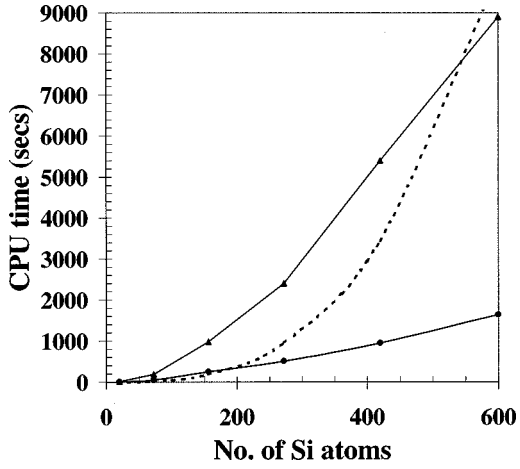

FIG. 9. CPU time for calculating a ground-state observable for 2D semiconductor (puckered-sheet polysilyne). Dashed line: Time of calculation based on diagonalization. Triangles: Time of the $D=4$ Chebyshev expansion method with 270 terms; Circles: Time of the one-step $D=4$ ERG method. Lines are a guide to the eye. All calculations are on a single processor of Cray T3E.

C. 2D Semiconductor: Puckered-sheet polysilyne $(SiH)_n$

An additional example of the power of the ERG method is shown in Fig. 9 where the CPU times for calculating an observable, such as the electronic energy of the ground state, is shown. The system is a puckered sheet of silicon atoms with hydrogen atoms above and below the sheet for stabilizing silicon dangling bonds. Additional hydrogen is introduced on the boundary of the sheet where silicon has two dangling bonds. This system is a semiconductor with a calculated[61] indirect gap of 2.48 eV.

The calculations are based on a tight-binding model of Goodwin *et al.*[62] and Kim *et al.*[63] The full set of parameters we used are given in Table II. The reader is referred to Ref. 63 for definition of the symbols in the table.

TABLE II. The tight binding parameters for polysilyne (Refs. 62–64).

	H–H	Si–H	Si–Si
$V_{ss\sigma}$ (eV)	−7.59	−3.5535	−1.82
$V_{sp\sigma}$ (eV)		5.088	1.96
$V_{pp\sigma}$ (eV)			3.06
$V_{pp\pi}$ (eV)			−0.87
r_0 ( )	0.742	1.48	2.35
r_c ( )	1.6	2.186	3.67
n	2.18	1.9877	2
n_c	14.0	13.269	6.48
m	4.215	2.255	4.54
m_c	3.50	3.01	6.48
U (eV)	3.15	5.795	3.5481
E_s (Si) (eV)	−13.08		
E_p (Si) (eV)	−4.785		
E_s (H) (eV)	−8.34		

This TB model underestimates the gap, yielding about 1.6 eV depending on system size. The energy range of the TB Hamiltonian is $\Delta E = 0.45$ a.u. The small gap is manifested in long-range DM correlations. A Chebyshev expansion calculation tuned to $D=4$ accuracy uses an inverse temperature of $\beta = 310$ and an expansion length of $P=270$ terms. As seen in Fig. 9, this leads to a formidable calculation that reaches a full linear scaling regime only for very large number of atoms. This is a typical problem in small band gap semiconductors.

An effective solution is to use a one-step version of the ERG method. If the system was much larger (and, therefore, sparser), a two step or higher number of ERG recursion steps would be advantageous of course, but because of the two-dimensional nature this would require too much memory than presently available on our systems. Here, for example, we used $\beta = 40$ and $P=46$. The computational gain of one step ERG seen in Fig. 9 is very significant.

V. SUMMARY

A novel approach to electronic structure of large systems has been presented. Three themes characterize the proposed ERG method. The electronic structure problem is cast in terms of functions of the Hamiltonian. This functional approach is useful since Chebyshev expansions allow to implement the required functions. A second theme is the energy scaling transformations achieved using energy-functional filters. The third is the use of coarse grained Hilbert space to achieve a length scale renormalization, so that the DM can be decomposed into a sum of terms, each describing a different energy and length regime of the problem, and each is represented by a sparse matrix.

As is usual with RG approaches, infinite length scales are manifested as scaling transformation invariants while finite length scales decay to zero with increasing scaling transformations. This invariance of the scaled correlation length in metals allows to represent the DM as a series of sparse matrices in nested Hilbert spaces.

The ERG method is also useful for many related problems: Whenever the DM range is large (even if it is finite); allows to significantly shorten the Chebyshev expansion length needed for resolving a small HOMO–LUMO gaps or for reaching high accuracy calculations.

ACKNOWLEDGMENTS

We thank Dr. Paul Maslen for introducing us to Ref. 65. This work was supported by Laboratory Directed Research and Development Program of Lawrence Berkeley Laboratory US-DOE contract No. DE-AC03-76SF00098. M.H.G. is a Packard Fellow.

APPENDIX

In this Appendix we discuss the origin of Eq. (17). It can be shown[65] that the following iterations ($k=0,1,2,...$):

$$W_{k+1}=\tfrac{1}{2}(3W_k - W_k Y_k W_k), \quad Y_{k+1}=\tfrac{1}{2}(3Y_k - Y_k W_k Y_k),$$

$$W_0 = -\sqrt{\alpha} I, \quad Y_0 = -\sqrt{\alpha} S, \quad \alpha^{-1} = N \max_{i,j} |S_{ij}|,$$

(where S is the positive definite $N\times N$ overlap matrix) converge quadratically to

$$W_\infty = -S^{-1/2}, \quad Y_\infty = -S^{1/2}.$$

For best linear scaling results, it is important that the matrices W and Y remain as sparse as possible. However, it is well-known that $S^{-1/2}$ is much less sparse than S itself, especially if S has a large condition number. On the other hand, the matrix $S^{1/2}$ is not really needed. We only need to calculate the matrix $H = S^{-1/2} R S^{-1/2}$ where $R = \mathbb{G}^T H^{(n)} \mathbb{G}$ is considerably sparse. It is, therefore, beneficial to calculate H directly and avoid at least part of the nonsparsity of $S^{-1/2}$. Towards this end, define the sequence of symmetric matrices ($k=0,1,2...$)

$$A_k = W_k H W_k, \quad B_k = Y_k W_k - 1,$$

it is straightforward to show that

$$A_{k+1} = A_k - (A_k B_k + B_k A_k)/2 + B_k A_k B_k/4,$$

$$B_{k+1} = (B_k - 3) B_k^2/4.$$

Thus quadratically converging to

$$A_\infty = S^{-1/2} H S^{-1/2}, \quad B_\infty = 0.$$

Numerical test of this procedure shows that the number of iterations is on the order of 10 and depends on the condition number of S. Furthermore, the matrices B_k start out from very sparse matrices and end as the zero matrix but in the interim iterations they become considerably less sparse. Yet, we have found that this scheme still leads to matrices more sparse matrices than the direct computation of $S^{-1/2}$.

[1] W. Kohn and L. J. Sham, Phys. Rev. B **140**, 1133 (1965).
[2] P. Hohenberg and W. Kohn, Phys. Rev. B **136**, 864 (1964).
[3] C. Z. Wang and K. M. Ho, Adv. Chem. Phys. **93**, 651 (1996).
[4] W. Yang, Phys. Rev. Lett. **66**, 1438 (1991).
[5] W. Yang, J. Chem. Phys. **94**, 1208 (1991).
[6] Q. Zhao and W. Yang, J. Chem. Phys. **102**, 9598 (1995).
[7] G. Galli and M. Parrinello, Phys. Rev. Lett. **69**, 3547 (1992).
[8] F. Mauri, G. Galli, and R. Car, Phys. Rev. B **47**, 9973 (1993).
[9] F. Mauri and G. Galli, Phys. Rev. B **50**, 4316 (1994).
[10] P. Ordejon, D. A. Drabold, M. P. Grumbach, and R. M. Martin, Phys. Rev. B **48**, 14646 (1993).
[11] P. Ordejon, D. A. Drabold, R. M. Martin, and M. P. Grumbach, Phys. Rev. B **51**, 1456 (1995).
[12] J. Kim, F. Mauri, and G. Galli, Phys. Rev. B **52**, 1640 (1995).
[13] W. Hierse and E. Stechel, Phys. Rev. B **50**, 17811 (1994).
[14] E. B. Stechel, A. R. Williams, and P. J. Feibelman, Phys. Rev. B **49**, 10088 (1994).
[15] E. Hernandez and M. J. Gillan, Phys. Rev. B **51**, 10157 (1995).
[16] W. Yang, Phys. Rev. B **56**, 9294 (1997).
[17] S. Goedecker and L. Colombo, Phys. Rev. Lett. **73**, 122 (1994).
[18] S. Goedecker and M. Teter, Phys. Rev. B **51**, 9455 (1995).
[19] R. Baer and M. Head-Gordon, J. Chem. Phys. **107**, 10003 (1997).
[20] U. Stephan and D. A. Drabold, Phys. Rev. B **57**, 6391 (1998).
[21] A. Voter, J. Kress, and R. Silver, Phys. Rev. B **53**, 12733 (1996).
[22] R. Silver, H. Roeder, A. Voter, and J. Kress, J. Comp. Physiol. **124**, 115 (1996).
[23] X.-P. Li, R. W. Nunes, and D. Vanderbilt, Phys. Rev. B **47**, 10891 (1993).
[24] M. S. Daw, Phys. Rev. B **47**, 10895 (1993).
[25] R. W. Nunes and D. Vanderbilt, Phys. Rev. B **50**, 17611 (1994).
[26] S-Y. Qui, C. Wang, K. Ho, and C. Chan, J. Phys.: Condens. Matter **6**, 9153 (1994).
[27] W. Kohn, Phys. Rev. Lett. **76**, 3168 (1996).
[28] S. Goedecker, Rev. Mod. Phys. (submitted).
[29] C. A. White, B. G. Johnson, P. M. W. Gill, and M. Head-Gordon, Chem. Phys. Lett. **230**, 8 (1994).

[30] M. C. Strain, G. E. Scuseria, and M. J. Frisch, Science **271**, 5245 (1996); **271**, 51 (1996); **271**, 52 (1996); **271**, 53 (1996).
[31] E. Schwegler, M. Challacombe, and M. Head-Gordon, J. Chem. Phys. **106**, 9708 (1997).
[32] C. Ochsenfeld, C. White, and M. Head-Gordon, J. Chem. Phys. **109**, 1663 (1998).
[33] D. M. York, T-S. Lee, and W. Yang, Chem. Phys. Lett. **263**, 297 (1996).
[34] J. Li and S. Yip, Phys. Rev. B **56**, 3524 (1997).
[35] S. Nomura, T. Iitaka, X. Zhao, T. Sugano, and Y. Aoyagi, Phys. Rev. B **56**, 4348 (1997).
[36] S. Itoh, P. Ordejon, D. A. Drabold, and R. M. Martin, Phys. Rev. B **53**, 2132 (1996).
[37] C. H. Xu and G. E. Scuseria, Chem. Phys. Lett. **262**, 219 (1996).
[38] W. Kohn, Phys. Rev. **115**, 809 (1959).
[39] J. des Cloizeaux, Phys. Rev. A **135**, 685 (1964); **135**, 698 (1964).
[40] A. Nenciu and G. Nenciu, Phys. Rev. B **47**, 10112 (1993).
[41] R. Baer and M. Head-Gordon, Phys. Rev. Lett. **79**, 3962 (1997).
[42] P. Maslen, C. Ochsenfeld, C. White, M. Lee, and M. Head-Gordon, J. Phys. Chem. **102**, 2215 (1998).
[43] S. Ismail-Beigi and T. Arias, Phys. Rev. B **57**, 11923 (1998).
[44] S. Goedecker, Phys. Rev. B **58**, 3501 (1998).
[45] P. W. Anderson, Phys. Rev. **109**, 1492 (1958).
[46] G. A. Baraf and M. Schluter, Phys. Rev. B **30**, 3460 (1984).
[47] C. Z. Wang, C. T. Chan, and K. M. Ho, Phys. Rev. Lett. **66**, 189 (1991).
[48] D. M. C. Nicholson, G. M. Stocks, Y. Wang, W. A. Shelton, Z. Stock, and W. M. Tennerman, Phys. Rev. B **50**, 14686 (1994).
[49] R. Haydock and R. L. Te, Phys. Rev. B **49**, 10845 (1994).
[50] Y. Wang, G. M. Stocks, W. A. Shelton, D. M. C. Nicholson, Z. Szotek, and W. M. Timmerman, Phys. Rev. Lett. **75**, 2867 (1995).
[51] K. G. Wilson, Rev. Mod. Phys. **47**, 773 (1975).
[52] R. Shankar, Rev. Mod. Phys. **66**, 129 (1994).
[53] S. R. White and R. M. Noack, Phys. Rev. Lett. **68**, 3487 (1992).
[54] S. R. White, Phys. Rev. B **48**, 10345 (1993).
[55] R. Kosloff and H. Tal-Ezer, Chem. Phys. Lett. **127**, 223 (1986).
[56] D. Neuhauser, J. Chem. Phys. **93**, 2611 (1990).
[57] M. R. Wall and D. Neuhauser, J. Chem. Phys. **102**, 8011 (1995).
[58] G. H. Golub and C. F. Van Loan, *Matrix Computations*, 3rd ed. (John Hopkins University Press, 1996).
[59] X. Blase, L. X. Benedict, E. L. Shirley, and S. G. Louie, Phys. Rev. Lett. **72**, 1878 (1994).
[60] Y. Wang and C. H. Mak, Chem. Phys. Lett. **235**, 37 (1995).
[61] K. Takeda and K. Shiraishi, Phys. Rev. B **39**, 11028 (1989).
[62] L. Goodwin, A. J. Skinner, and D. G. Pettifor, Europhys. Lett. **9**, 1701 (1989).
[63] E. Kim, Y. H. Lee, and J. M. Lee, J. Phys.: Condens. Matter **6**, 9561 (1994).
[64] E. Kim, private communication (1998).
[65] V. B. Larin, Technicheskaya Kibernetika **1**, 210 (1992).